A UNIFIED APPROACH TO THE STUDY OF TURBULENCE OVER SMOOTH AND DRAG-REDUCING SURFACES

Joseph I. Ibrahim, Garazi Gómez-de-Segura and Ricardo García-Mayoral
Department of Engineering
University of Cambridge
Trumpington St, Cambridge CB2 1PZ, UK
r.gmayoral@eng.cam.ac.uk

ABSTRACT

We investigate the effect that drag-reducing surfaces of small texture size have on the dynamics of near-wall turbulence. Luchini *et al.* (1991) proposed that the effect of these surfaces on the flow could be reduced to setting virtual origins for the streamwise and spanwise velocity components. We conduct direct numerical simulations of turbulent channel flows and extend this idea by imposing different virtual origins for all three velocity components using Robin, slip-length-like boundary conditions. We show that the virtual origin for the mean flow is set by the streamwise slip length, while that for the turbulence, embodied by the quasi-streamwise vortices of the near-wall cycle, is set by the wall-normal and spanwise slip lengths. We demonstrate that the outward shift in the mean velocity profile is simply the difference between these two virtual origins, and derive an expression that can be used to predict the virtual origin for turbulence a priori. We show that, other than by the shift in origin, the turbulence remains essentially smooth-wall-like.

INTRODUCTION

Certain complex surfaces, such as riblets, superhydrophobic surfaces or anistropic permeable substrates, consist of small surface modifications, or texture, and are designed to manipulate the flow to achieve a reduction in turbulent skin-friction drag. Like many turbulent-flow control techniques, including active ones, they aim to manipulate the near-wall cycle due to its key role in the generation of turbulent skin friction. For drag-reducing surfaces of small texture size, the net effect can be thought of as a relative displacement of the quasi-streamwise vortices away from the surface with respect to the mean flow. This reduces the local turbulent mixing of streamwise momentum and, therefore, the skin-friction drag.

Provided that surface manipulations are small, the direct effect of the texture is confined to the near-wall region, and the change in drag is manifested in a constant shift of the mean velocity profile, ΔU^+, experienced by the flow above the near-wall region (Clauser, 1956). For sufficiently small textures, this is caused by the flow perceiving the surface in a homogenised fashion. In this paper, x, y and z refer to the streamwise, wall-normal and spanwise coordinates, respectively, and u, v and w are their corresponding velocity components. The mean streamwise velocity is U, and the superscript '+' denotes normalisation in viscous units.
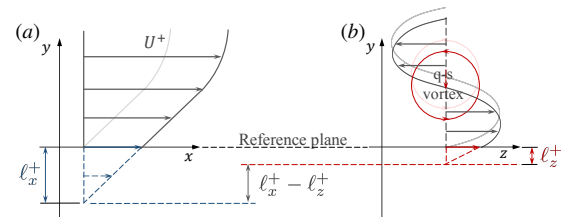

Figure 1. Schematic of (*a*) streamwise and (*b*) spanwise slip lengths, ℓ_x^+ and ℓ_z^+, and the corresponding virtual origins at $y^+ = -\ell_x^+$ and $y^+ = -\ell_z^+$. A quasi-streamwise vortex (q-s vortex), inducing a spanwise velocity w^+, is sketched in (*b*).

For riblets, Bechert & Bartenwerfer (1989) originally suggested that the mean streamwise flow experiences an apparent, no-slip wall, or virtual origin, at a depth ℓ_x below the riblet tips, which they called the 'protrusion height'. This is depicted in figure 1(*a*). Defining, for convenience, the reference plane $y = 0$ to be located at the riblet tips, this would be equivalent to a Navier slip condition of the form $u = \ell_x \partial u/\partial y$. However, the spanwise velocity near the surface, induced by the quasi-streamwise vortices of the near-wall cycle, would not, in general, perceive an origin at the riblet tips, $y = 0$. Luchini *et al.* (1991) proposed, therefore, that it would also be necessary to consider a spanwise slip length, ℓ_z, to properly describe the full effect of riblets on the flow. The spanwise velocity would then perceive a virtual origin at a distance ℓ_z below the riblet tips, as shown in figure 1(*b*), which would be equivalent to $w = \ell_z \partial w/\partial y$ at $y = 0$. Luchini *et al.* (1991) concluded that the only important parameter in determining the drag reduction would be the difference between these two virtual origins, i.e. $\ell_x - \ell_z$. It has since been proposed that $\Delta U^+ \propto \ell_x^+ - \ell_z^+$ (Jiménez, 1994; Luchini, 1996), which is valid for $\ell_x^+, \ell_z^+ \lesssim 1$, with a constant of proportionality between 0.6 and 1, depending on the author (see also Bechert *et al.*, 1997). Increasing ℓ_x^+ increases the relative offset between the mean flow and the quasi-streamwise vortices, reducing the drag, while increasing ℓ_z^+ has the opposite effect.

However, when the spanwise slip length generated by a surface becomes larger than a few wall units, the drag-increasing effect of ℓ_z^+ on ΔU^+ starts to saturate (Busse & Sandham, 2012). Fairhall & García-Mayoral (2018)
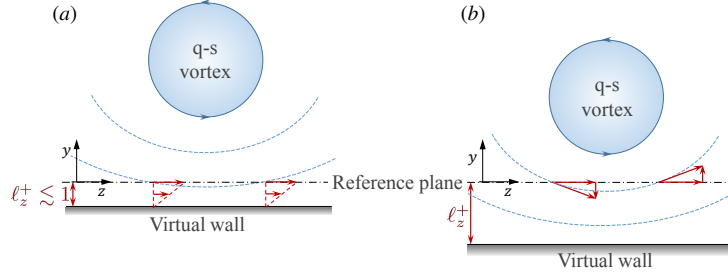
Figure 2. Schematic of spanwise and wall-normal velocities induced by quasi-streamwise vortices at the reference plane for (a) virtual origins $\ell_z^+ \lesssim 1$ and (b) larger virtual origins.

showed that this saturation can be accounted for with an 'effective' spanwise slip length, $\ell_{z,eff}^+$, which is empirically observed to be

$$\ell_{z,eff}^+ \approx \frac{\ell_z^+}{1 + \ell_z^+/4} \qquad (1)$$

The change in drag would then be $\Delta U^+ \propto \ell_x^+ - \ell_{z,eff}^+$.

Gómez-de-Segura et al. (2018a) have recently investigated the cause for this saturation in the drag-increasing effect of ℓ_z^+ (1). The underlying assumption of the linear law, $\Delta U^+ \propto \ell_x^+ - \ell_z^+$, is that the only effect of the quasi-streamwise vortices is to induce a Couette-like, transverse shear at the reference plane $y = 0$, but no wall-normal velocity. This is valid as long as $\ell_z^+ \lesssim 1$, since w is linear just above the wall, whereas v is quadratic. In this regime, the effect of the surface on the flow would be captured by the conditions $u = \ell_x \partial u / \partial y$, $w = \ell_z \partial w / \partial y$ and $v = 0$ at $y = 0$. However, as ℓ_z^+ is increased and the vortices approach the reference plane further, the assumption of impermeability is no longer valid, as depicted in figure 2. Gómez-de-Segura et al. (2018a) argued, therefore, that the displacement, on average, of the quasi-streamwise vortices towards the reference plane would necessarily saturate, unless the shift of the origin perceived by w was also accompanied by a shift of the origin perceived by v. They conducted preliminary simulations in order to find a suitable method for imposing a virtual origin for v through an equivalent boundary condition. The most successful was a Robin condition, $v = \ell_y \partial v / \partial y$, which takes the same form as the slip conditions for u and w discussed above, even if it does not convey the same physical meaning. When a virtual origin for v consistent with that for w is imposed, the saturation in the effect of ℓ_z^+ no longer occurs. This suggests that, in general, to fully describe the effects of a complex surface on the flow, it is necessary to consider virtual origins for all three velocity components, because the virtual origin for v also plays an important role in the apparent origin for the quasi-streamwise vortices.

The above suggests that when the virtual origins perceived by v and w differ, the quasi-streamwise vortices, and hence the turbulence, will perceive a virtual origin at some intermediate plane between the two (Gómez-de-Segura et al., 2018a; García-Mayoral et al., 2019). Let us assume, then, that the only effect of the virtual origins, particularly those perceived by v and w, on the near-wall turbulence is to set its origin at some intermediate plane $y^+ = -\ell_T^+$, while the flow remains otherwise smooth-wall-like. We will refer to this plane as the virtual origin for turbulence. From the mean streamwise momentum equation, the shape of the mean velocity profile is determined by the turbulence through the Reynolds stress. If the only
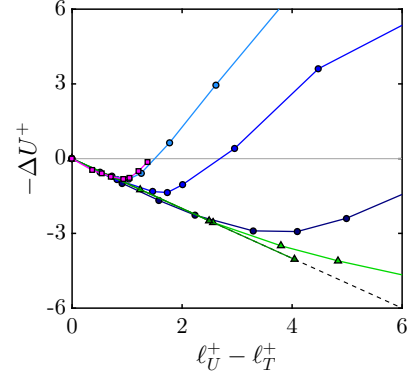

Figure 3. ΔU^+ for various types of complex surfaces as a function of the difference between the virtual origins $\ell_U^+ - \ell_T^+$. Adapted from Gómez-de-Segura et al. (2018b). —□—, riblets; —○—, from light to dark blue, permeable substrates with increasing streamwise to wall-normal permeability ratios; —△—, superhydrophobic surfaces with regular and randomly distributed posts.

effect of the virtual origins on the turbulence, and hence the Reynolds stress, is to shift its origin to $y^+ = -\ell_T^+$, then the only change to the mean velocity profile compared to that over a smooth wall would simply be a shift by its value at $y^+ = -\ell_T^+$. If the mean velocity profile perceives an origin at $y^+ = -\ell_U^+$, then the outward shift of the mean velocity profile above the plane $y^+ = -\ell_T^+$ would then necessarily be given by (García-Mayoral et al., 2019)

$$\Delta U^+ = \ell_U^+ - \ell_T^+ \qquad (2)$$

Equation (2) holds as long as the only effect of the texture on the turbulence is to change the virtual origin that it perceives, and not the dynamics of the near-wall cycle. This requires that the texture size is small in wall units (García-Mayoral et al., 2019). Figure 3 demonstrates that, for real textured surfaces, when the texture size becomes too large, there is an eventual departure from the linear relationship between ΔU^+ and the difference $\ell_U^+ - \ell_T^+$, and the flow no longer perceives the surface in a homogenised fashion.

The aim of the present work is to study, for surfaces that impose different virtual origins for the different velocity components, whether this effect can be reduced to simply setting the virtual origins perceived by the mean flow and the turbulence. If this is the case, then the shift in the mean velocity profile, ΔU^+, will be described by (2). We do this by conducting direct numerical simulations of turbulent

2

Table 1.   Summary of simulations, including the slip lengths used for the boundary conditions, ℓ_x^+, ℓ_z^+ and ℓ_y^+, and their corresponding virtual origins calculated a priori from the smooth-wall profiles, ℓ_u^+, ℓ_w^+ and ℓ_v^+. The virtual origin for turbulence, ℓ_T^+, is measured a posteriori and compared to that predicted by equation (4), $\ell_{T,pred}^+$. The slip length for the mean flow, $\ell_{x,m}^+$ is given only when it is different to the slip length for the streamwise velocity fluctuations. In the simulation labels, 'U', 'V' and 'W' denote a non-zero slip-length boundary condition on u, v and w, respectively, and 'F' denotes slip applied to the streamwise velocity fluctuations only, i.e. $\ell_{x,f}^+ > 0$ and $\ell_{x,m}^+ = 0$.

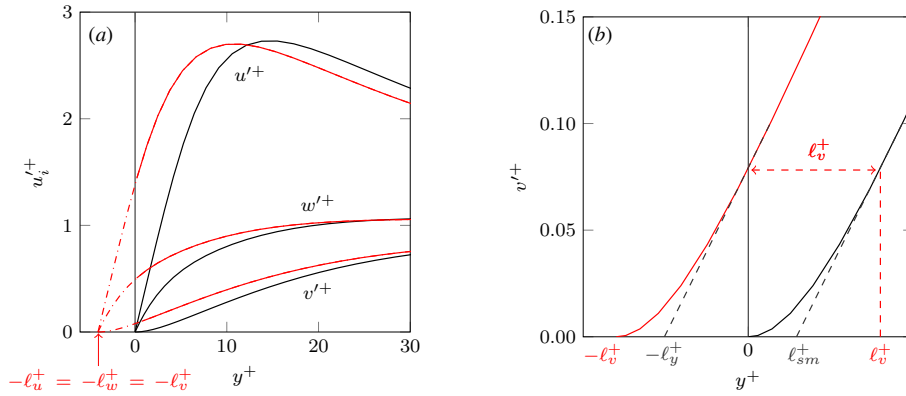| Case	ℓ_x^+	ℓ_z^+	ℓ_y^+	$\ell_{x,m}^+$	ℓ_u^+	ℓ_w^+	ℓ_v^+	ℓ_T^+	$\ell_{T,pred}^+$
UV1	2.0	0.0	1.2	-	2.0	0.0	2.2	0.0	0.0
UWV1	2.0	2.0	1.2	-	2.0	1.7	2.2	1.7	1.7
UWV2	4.0	4.0	1.2	-	3.6	2.9	2.2	2.7	2.8
UWV3	4.0	4.0	2.5	-	3.6	2.9	4.0	3.0	2.9
UWV4	4.0	6.0	1.5	-	3.6	4.1	2.5	3.6	3.7
UWV5	4.0	6.0	2.0	-	3.6	4.1	3.2	3.8	4.0
UWV6	4.0	6.0	2.2	10	3.6	4.1	3.9	4.0	4.1
F1–F6	$5.0 - \infty$	0.0	0.0	0.0	$4.2 - \infty$	0.0	0.0	0.0	0.0

Figure 4.   Schematics showing (*a*) the definition of virtual origins ℓ_u^+, ℓ_v^+ and ℓ_w^+ as the shift of the rms velocity fluctuations with respect to a smooth channel (black lines), and (*b*) the difference between ℓ_v^+ and ℓ_y^+, $\ell_y^+ = \ell_v^+ - \ell_{sm}^+$.

channel flows and impose different virtual origins for each velocity component using Robin slip-length boundary conditions. We then assess whether the effect of virtual origins on the turbulence can be accounted for by a single parameter, ℓ_T^+, and whether ℓ_T^+ can be predicted from the virtual origins perceived by the different velocity components.

NUMERICAL METHOD

We carry out direct numerical simulations of turbulent channel flows at a friction Reynolds number $\mathrm{Re}_\tau \approx 180$ in a doubly-periodic box in the wall-parallel directions, using a code adapted from García-Mayoral & Jiménez (2011). In all cases, the channel half-height is $\delta = 1$ and the domain size is $L_x = 2\pi\delta$, $L_y = 2\delta$ and $L_z = \pi\delta$ in each respective coordinate direction. Virtual origins for the three velocity components are introduced by imposing Robin boundary conditions at the channel walls, the method also used by Gómez-de-Segura *et al.* (2018*a*). These take the form $u = \ell_x \partial u/\partial y$, $v = \ell_y \partial v/\partial y$ and $w = \ell_z \partial w/\partial y$, where ℓ_x, ℓ_y and ℓ_z are the slip lengths in the streamwise, wall-normal and spanwise directions, respectively. As mentioned above, ℓ_y does not convey a slip effect for v, but, by extension,

we will refer to ℓ_y as the 'slip length' in the wall normal direction in the present study. From continuity, the slip length for the mean wall-normal velocity is set to zero, since there can be no transpiration on average through the surface, and hence the slip length is applied only to the fluctuating component v'. Note also that a free-slip condition, e.g. $\partial u/\partial y = 0$, is equivalent to having an infinitely large slip length, ℓ_x.

While the concepts of slip lengths and virtual origins have been used interchangeably in the literature, here we make a distinction between the two terms. The slip lengths ℓ_x^+, ℓ_y^+ and ℓ_z^+ are defined exclusively as the Neumann coefficients for the simulation boundary conditions. Physically, they simply correspond to the y-locations where the velocity components become zero when linearly extrapolated from the reference plane. In contrast, we define the virtual origins of u, v and w as the locations below the reference plane where each velocity component would perceive a virtual, smooth wall. These correspond to the heights at which the profiles of the rms velocity fluctuations u'^+, v'^+ and w'^+ would go to zero assuming that the shape of each profile remains smooth-wall-like independently of the others, and would be located at $y^+ = -\ell_u^+$, $y^+ = -\ell_v^+$ and
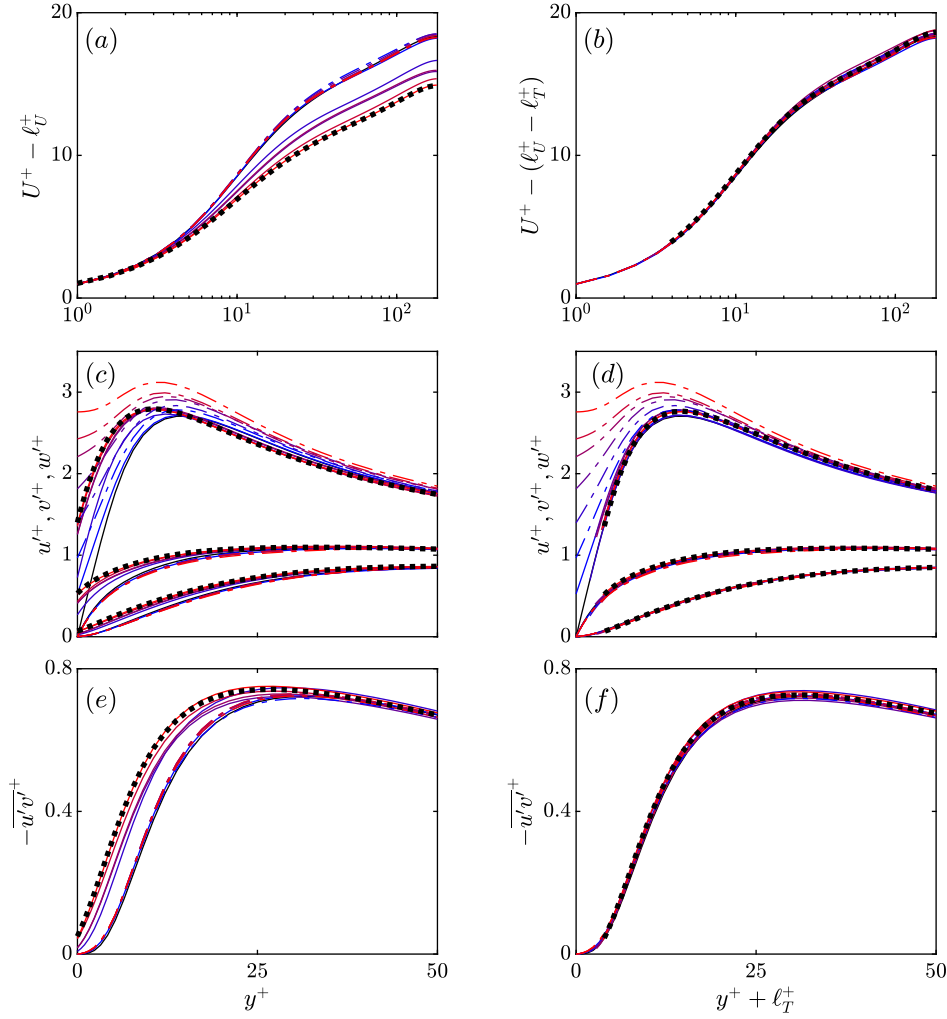
Figure 5. Mean velocity profiles, rms velocity fluctuations and Reynolds stress profiles for simulations with slip and tran-spiration, compared to the smooth-wall reference case (black lines). (a,c,e), scaled with u_τ at the plane where the boundary conditions are imposed, $y^+ = 0$. (b,d,f), scaled with u_τ at the origin perceived by the turbulence, $y^+ = -\ell_T^+$, and shifted in y^+ by ℓ_T^+. Solid lines, from blue to red, Cases UV1 and UWV1–UVW5; dash-dot lines, from blue to red, Cases F1–F6; black dotted line, Case UWV6. See table 1 for details. Note that all curves in (a), (c) and (e) are included in (b), (d) and (f).

$y^+ = -\ell_w^+$, respectively. The definition of these virtual origins is also portrayed in figure 4(a). We therefore choose the slip lengths according to the virtual origins we wish to impose. A summary of the simulations we have conducted in this study is given in table 1.

For a virtual origin of a few wall units, we expect the slip lengths ℓ_x^+ and ℓ_z^+ to be approximately equal to the virtual origins ℓ_u^+ and ℓ_w^+, because the wall-parallel velocities u^+ and w^+ are approximately linear in the immediate vicinity of the wall. The case of v, however, is more subtle. Since v' is quadratic near the wall, the height of the virtual origin perceived by v, $y^+ = -\ell_v^+$, can differ significantly from the slip length ℓ_y^+, even for small values. We choose ℓ_y^+ by matching the ratio between v^+ and $\partial v^+/\partial y^+$ at a height $y^+ = \ell_v^+$ above a smooth wall. From figure 4(b), ℓ_y^+ and ℓ_v^+ are related by $\ell_y^+ = \ell_v^+ - \ell_{sm}^+$, where ℓ_{sm}^+ is obtained by extrapolating the slope of the smooth-wall profile at $y^+ = \ell_v^+$. Finally, it should be noted that a similar curvature effect can also be significant for ℓ_w^+, since the profile of w'^+ becomes noticeably curved for $y^+ \gtrsim 2$, but this effect is small for ℓ_u^+.

RESULTS

We carry out simulations for a range of combinations of ℓ_x^+, ℓ_y^+ and ℓ_z^+, and compute a priori the virtual origins ℓ_u^+, ℓ_v^+ and ℓ_w^+, assuming the shape of smooth-wall velocity profiles remain unchanged. It should be noted that there is a one-to-one relationship between slip lengths and virtual origins. The virtual origins are included alongside the slip lengths in table 1. The mean velocity profiles, rms velocity fluctuations and Reynolds stress profiles for these simulations are included in figure 5. The figure shows that when the wall-normal coordinate is measured from the virtual origin for turbulence, $y^+ + \ell_T^+ = 0$, with u_τ defined at the same height from the total-stress curve, the wall-normal and spanwise rms fluctuations and Reynolds stress curves essentially collapse to the smooth-wall data. The origin for turbulence, ℓ_T^+, is measured a posteriori by finding the shift that best fits the Reynolds stress curve in the near-wall region for $5 \lesssim y^+ + \ell_T^+ \lesssim 20$ to smooth-wall data. This is also included in table 1 for each case. Our results suggest that the turbulence experiences a virtual origin intermediate between ℓ_v^+ and ℓ_w^+ when $0 < \ell_v^+ < \ell_w^+$. On the other hand, when $\ell_v^+ \geq \ell_w^+$ we observe that $\ell_T^+ \approx \ell_w^+$. The reasons for this will be discussed later.
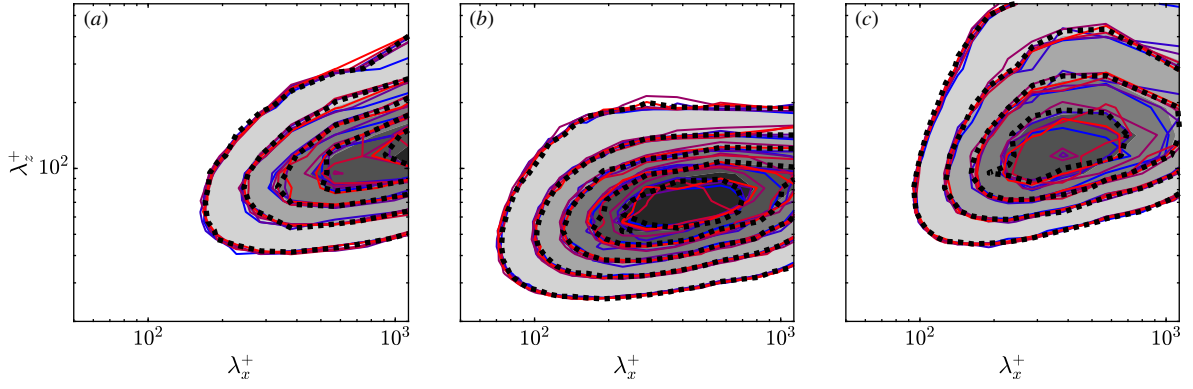
4

Figure 6. Premultiplied two-dimensional spectral densities of u^2, v^2 and w^2, plotted at $y^+ + \ell_T^+ \approx 15$ and scaled with u_τ measured at the origin for turbulence, $y^+ = -\ell_T^+$. Shaded contours, smooth-wall data; solid lines, blue to red, Cases UV1 and UWV1–UWV5; black dotted line, Case UWV6. (a) $k_x k_z E_{uu}$; (b) $k_x k_z E_{vv}$; (c) $k_x k_z E_{ww}$. The contour increments in wall units are 0.3225, 0.0099 and 0.0393 for (a–c), respectively.
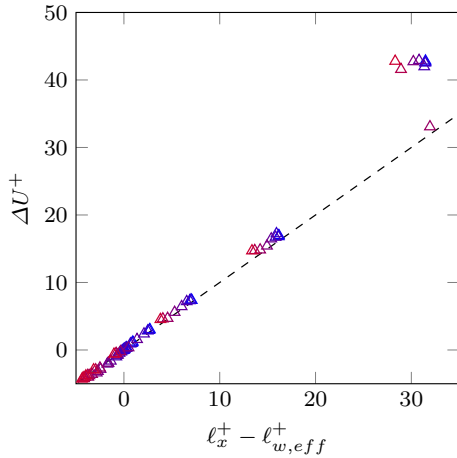

Figure 7. ΔU^+ as a function of $\ell_x^+ - \ell_{w,eff}^+$, where $\ell_{w,eff}^+$ is given by (3). Simulations at $Re_\tau = 180$. From blue to red, the spanwise slip length, and hence ℓ_w^+, increases. The dashed line represents $\Delta U^+ = \ell_x^+ - \ell_{w,eff}^+$. Data obtained from Busse & Sandham (2012).

Figure 5(b) also demonstrates that the mean velocity profile collapses to the smooth-wall case, save for a shift $\Delta U^+ = \ell_U^+ - \ell_T^+$, where ℓ_U^+ is the distance between the virtual origin experienced by the mean flow and the plane $y = 0$. This supports the validity of equation (2). The collapse of the mean velocity, rms fluctuation and Reynolds stress profiles to the smooth-wall data indicates that the near-wall turbulent dynamics remain smooth-wall-like, and that ℓ_T^+ fully describes the effect of virtual origins on turbulence (García-Mayoral et al., 2019). Figure 6 portrays the premultiplied energy spectra at $y^+ + \ell_T^+ \approx 15$ for several cases along with that of a smooth-wall flow at $y^+ \approx 15$, and supports the idea that the near-wall turbulent dynamics remain essentially smooth-wall-like.

The expression for ΔU^+ does not depend explicitly on the virtual origin experienced by the streamwise velocity fluctuations, but rather on the virtual origin experienced by the mean flow, ℓ_U^+. We also argue that ℓ_T^+ depends only on ℓ_v^+ and ℓ_w^+. This suggests that the virtual origin experienced by the mean flow may be independent of that experienced by the streamwise velocity fluctuations, and that the

only streamwise origin relevant to ΔU^+ is, in fact, ℓ_U^+. To demonstrate this, one of the cases included in figure 5 has a larger slip length on the mean flow ($\ell_{x,m}^+ = 10$) than on the streamwise fluctuations ($\ell_{x,f}^+ = 4$). The figure shows that $\Delta U^+ = \ell_U^+ - \ell_T^+$, and $\ell_{x,m}$ has no influence on the turbulent fluctuations or Reynolds stress. To further test this, we conduct simulations with a slip length applied to the streamwise velocity fluctuations only, varying from $\ell_{x,f}^+ = 5$ to infinity, with no slip on the mean flow. The results for these simulations are also presented in figure 5. While the peak value of the rms streamwise velocity fluctuations exhibits a gradual increase with increasing slip length, this has a negligible effect on the mean velocity profile, and ΔU^+ remains essentially zero. The reason for this is that as ℓ_x^+ is increased, the streamwise velocity fluctutations experience a deeper virtual origin and can therefore decay pseudo-linearly to zero more slowly, as shown in 5(d). This changes their slope in the vicinity of the plane $y = 0$ and is the likely cause for the gradual increase in the peak value of u'^+. However, because the origins for the mean, wall-normal and spanwise velocities remain at $y = 0$, this has no effect on ΔU^+.

Based on the results of our simulations, we propose an alternative form for the effective spanwise slip length (1), which takes into account that $\ell_w^+ \neq \ell_z^+$

$$\ell_{w,eff}^+ \approx \frac{\ell_w^+}{1 + \ell_w^+/5} \qquad (3)$$

Figure 7 shows the excellent agreement of ΔU^+ with the difference $\ell_x^+ - \ell_{w,eff}^+$. Equation (3) therefore provides an expression to predict ℓ_T^+ when $\ell_v^+ = 0$. However, we have observed that ℓ_T^+ also depends on ℓ_v^+. As demonstrated by Gómez-de-Segura et al. (2018a), if $\ell_v^+ \approx \ell_w^+$ then no saturation in the effect of ℓ_w^+ occurs and $\ell_T^+ \approx \ell_w^+$. If we increase ℓ_v^+ further, such that $\ell_v^+ > \ell_w^+$, we would not expect the quasi-streamwise vortices to approach the surface further, since their first-order effect is to induce a spanwise velocity at the reference plane. Even if v was allowed to penetrate freely through the reference plane, the quasi-streamwise vortices would require some amount of spanwise slip in the first place to approach this plane. Therefore, when $\ell_v^+ \geq \ell_w^+$, we would expect $\ell_T^+ \approx \ell_w^+$, which we observe in our simulations. On the other hand, in the regime where $0 < \ell_v^+ < \ell_w^+$, it should be possible to predict the virtual origin for turbu-
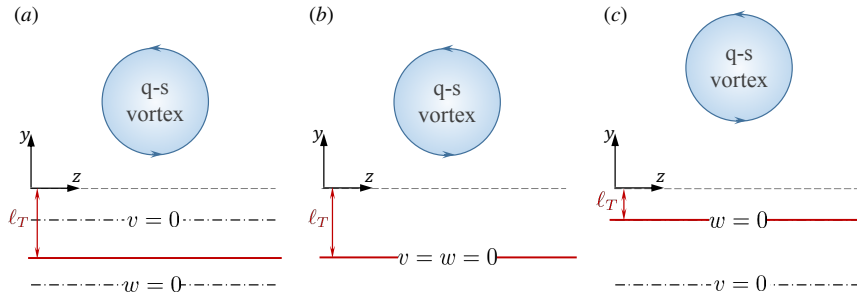
Figure 8. Schematics of the location of the origin for turbulence, $y^+ = -\ell_T^+$, when imposing different origins for the spanwise and wall-normal velocities. The planes where $v = 0$ and $w = 0$ correspond to the imposed virtual origins, $y^+ = -\ell_v^+$ and $y^+ = -\ell_w^+$, respectively. The origin for turbulence, $y^+ = -\ell_T^+$, is represented by the red line. (a) $\ell_v^+ < \ell_w^+$; (b) $\ell_v^+ = \ell_w^+$; (c) $\ell_v^+ > \ell_w^+$. Note that in each case, the distance between the centre of the quasi-streamwise vortices and the plane $y^+ = -\ell_T^+$ remains the same.

lence by simply changing the frame of reference of (3) to the virtual origin for v, i.e. $y^+ = -\ell_v^+$. This is because the saturation in the effect of ℓ_w^+ is a direct result of the plane at which v perceives an impermeable wall. A general expression for approximating ℓ_T^+ from ℓ_w^+ and ℓ_v^+ would then be

$$\ell_{T,pred}^+ \approx \begin{cases} \ell_v^+ + \dfrac{(\ell_w^+ - \ell_v^+)}{1 + (\ell_w^+ - \ell_v^+)/5} & \text{if } \ell_w^+ > \ell_v^+ \\ \ell_w^+ & \text{if } \ell_w^+ \le \ell_v^+ \end{cases} \quad (4)$$

The physical interpretation of (4) is sketched in figure 8. When $\ell_{T,pred}^+$ is predicted from the virtual origins ℓ_v^+ and ℓ_w^+ known a priori in our simulations, it shows very good agreement with the measured value of ℓ_T^+, as shown in table 1.

CONCLUSIONS

We have analysed the effect on turbulence of surfaces that impose different apparent virtual origins on the three velocity components. Examples of such surfaces are passive flow-control technologies, such as riblets or superhydrophobic surfaces. Our results show that the shift in the mean velocity profile, ΔU^+, is determined by the virtual origin experienced by the mean flow, ℓ_U^+, and the virtual origin experienced by the turbulence, ℓ_T^+, verifying equation (2). This analysis is valid for complex surfaces of small texture size. For the combinations of virtual origins imposed in our simulations, turbulence remains essentially smooth-wall-like, except for the shift ℓ_T^+. Through a combination of physical and empirical arguments it is possible to predict the virtual origin for turbulence a priori, and in general it lies between the virtual origins for the spanwise and wall-normal velocities, as expressed by equation (4). It is therefore possible to predict the shift in the mean velocity profile for a given complex surface using equations (2) and (4).

REFERENCES

Bechert, D. W. & Bartenwerfer, M. 1989 The viscous flow on surfaces with longitudinal ribs. *J. Fluid Mech.* **206**, 105–129.

Bechert, D. W., Bruse, M., Hage, W., van der Hoeven, J. G. T. & Hope, G. 1997 Experiments on drag-reducing surfaces and their optimization with an adjustable geometry. *J. Fluid Mech.* **338**, 59–87.

Busse, A. & Sandham, N. D. 2012 Influence of an anistropic slip-length boundary condition on turbulent channel flow. *Phys. Fluids* **24**, 055111.

Clauser, F. H. 1956 The turbulent boundary layer. *Adv. Appl. Mech.* **4**, 1–51.

Fairhall, C. T. & García-Mayoral, R. 2018 Spectral analysis of the slip-length model for turbulence over textured superhydrophobic surfaces. *Flow Turbul. Combust.* **100**, 961–978.

García-Mayoral, R., Gómez-de-Segura, G. & Fairhall, C. T. 2019 The control of near-wall turbulence through surface texturing. *Fluid Dyn. Res.* **51**, 011410.

García-Mayoral, R. & Jiménez, J. 2011 Hydrodynamic stability and breakdown of the viscous regime over riblets. *J. Fluid Mech.* **678**, 317–347.

Gómez-de-Segura, G., Fairhall, C. T., MacDonald, M., Chung, D. & Garicía-Mayoral, R. 2018*a* Manipulation of near-wall turbulence by surface slip and permeability. *J. Phys. Conf. Ser.* **1001**, 012011.

Gómez-de-Segura, G., Sharma, A. & García-Mayoral, R. 2018*b* Virtual origins in turbulent flows over complex surfaces. In *Proceedings of the 2018 Summer Program*, pp. 277–286. Stanford University: Centre for Turbulence Research.

Jiménez, J. 1994 On the structure and control of near wall turbulence. *Phys. Fluids* **6**, 944.

Luchini, P. 1996 Reducing the turbulent skin friction. In *Computational Methods in Applied Sciences '96*, pp. 466–470. John Wiley & Sons Ltd.

Luchini, P., Manzo, F. & Pozzi, A. 1991 Resistance of a grooved surface to parallel flow and cross-flow. *J. Fluid Mech.* **228**, 87–109.